J. Fluid Mech. (1983), *vol.* 130, *pp.* 13–26
Printed in Great Britain

Turbulence structure in stably stratified open-channel flow

By SATORU KOMORI, HIROMASA UEDA,
Division of Atmospheric Environment, The National Institute for Environmental Studies, Ibaraki 305, Japan

FUMIMARU OGINO AND TOKURO MIZUSHINA
Department of Chemical Engineering, Kyoto University, Kyoto 606, Japan

(Received 28 September 1979 and in revised form 7 December 1982)

The effects of stable stratification on turbulence structure have been experimentally investigated in stratified open-channel flow and a theoretical spectral-equation model has been applied to the stably stratified flow. The measurements were made in the outer layer of open-channel flow with strongly stable density gradient, where the wall effect was small. Velocity and temperature fluctuations were simultaneously measured by a laser-Doppler velocimeter and a cold-film probe. Measurements include turbulent intensities, correlation coefficients of turbulent fluxes and coherence–phase relationships. These turbulent quantities were correlated with the local gradient Richardson number and compared with the values calculated using a spectral-equation model and with other laboratory measurements. In stable conditions, turbulent motions approach wavelike motions, and negative heat and momentum transfer against the mean temperature and velocity gradient occurs in strongly stable stratification.

1. Introduction

Fluids appearing in the environment are in motion, and usually the flow is turbulent. In addition, since heat transfer on an environmental scale usually involves buoyancy effects, it is important to know the interaction between buoyancy and turbulence. One such flow configuration is stratified shear flow, which has been an important subject of study in the atmospheric boundary layer, the ocean and in many industrial operations. A large number of field investigations have been performed in the surface layer under stable conditions by many geophysicists: Wyngaard, Cote & Izumi (1971), Haugen, Kaimal & Bradley (1971), McBean & Miyake (1972) and others. Laboratory experiments have been performed by Webster (1964), Young (1975), Arya & Plate (1969), Arya (1975) and Piat & Hopfinger (1981) in wind tunnels and by Ellison & Turner (1960), Schiller & Sayre (1975), Mizushina *et al.* (1978) and Komori *et al.* (1982*a*) in open channels. Of these measurements, the field observations and some of the laboratory experiments (Arya & Plate 1969; Arya 1975) have been conducted in the stably stratified boundary-layer flow generated by cooling the wall or ground. In the stratified wall region or atmospheric surface layer with large temperature and velocity gradients, the turbulence shear-production rate is strongly affected by buoyancy, so that organized turbulent motions (bursting phenomena) are extremely changed. Contrary to such stratified flow, Webster's and Young's flows are grid-generated turbulent flows with vertical temperature and velocity gradients in the outer layer in specially designed wind tunnels. Mizushina *et al.* (1978) and Komori *et al.* (1982*a*) also conducted the experiments in the developed stratified outer-layer

flows generated by heating the top of the outer layer in an open channel, and Piat & Hopfinger (1981) measured the turbulence quantities in a developing stratified boundary layer generated by discharging the warm air above the cold lower stream in a wind tunnel. As discussed in a previous paper (Komori *et al.* 1982*b*), the stratified outer-layer flows are relatively free of wall effects and can be presumed to be close to a nominally homogeneous free shear flow in local equilibrium. Launder (1975) and Gibson & Launder (1978) showed theoretically that the local gradient Richardson number becomes a significant parameter for representing the stability in such a free shear flow in local equilibrium; energy production by the combined effects of mean shear and buoyancy being approximately balanced by viscous dissipation. Experimentally, Webster (1964), Young (1975), Mizushina *et al.* (1978) and Komori *et al.* (1982*a*) have confirmed that eddy diffusivities and some turbulence quantities are well correlated with the local gradient Richardson number. Ueda, Mitsumoto & Komori (1981) also observed the same stability dependences of eddy diffusivities in the atmospheric boundary layer above the surface layer as those obtained in the outer layer of a stratified open-channel flow (Mizushina *et al.* 1978). Although it is of interest for both an experimentalist and a theoretician to clarify the detailed structure of such stably stratified flow close to a free shear flow in local equilibrium, only a few investigations of the detailed structure have been performed.

The purpose of the present paper is to clarify in more detail the buoyancy effects on the turbulence structure in a developed stably stratified outer layer in open-channel flow. The present flow configuration is the same used in the previous works (Mizushina *et al.* 1978; Komori *et al.* 1982*a*), and it may be similar to that of Piat & Hopfinger (1981). Piat & Hopfinger (1981) investigated the effect of stratification on the distributions of turbulence quantities during the developing process of the boundary layer in a wind tunnel, whereas the present study was focused on the change of the turbulence structure due to buoyancy effects in a developed flow close to local equilibrium. To obtain the developed stable conditions, the present stratified flow was produced by heating the free surface (the top of the outer layer) of the open-channel flow in the region where the flow had been a fully developed flow under neutral conditions. In the developed stratified flow, turbulence quantites were measured and correlated by the local gradient Richardson number defined by $Ri = \beta g(\partial\overline{T}/\partial y)/(\partial\overline{U}/\partial y^2)$, where β is the expansion coefficient, g the gravitational acceleration, $\overline{T}$ the mean temperature, U the mean velocity and y the vertical distance from the wall. In order to attain a theoretical insight into the measurements, a spectral-equation model developed by Deissler (1958, 1967, 1971) was applied to a stably stratified shear flow with constant temperature and velocity gradients, and compared qualitatively with the experimental results.

2. Spectral-equation model

The present spectral-equation model is the same as that used in the papers by Deissler (1958, 1971) and the previous work (Komori *et al.* 1982*a*, *b*). The spectral-equation model is applicable to nominally homogeneous shear flow close to local equilibrium, and has an important advantage in the prediction of pressure correlations, which play a substantial role in the stratified flow but cannot be measured. The basic equations are the Navier–Stokes, energy and continuity equations for an incompressible flow with constant temperature and velocity gradients in the vertical direction. Under the assumptions of homogeneity and the neglect of triple

correlations, two-point correlation equations in the spectral form are written as

$$\underbrace{\frac{\partial E_{ij}}{\partial \tau}}_{\text{I}} = \underbrace{-\{\delta_{i1}E_{2j}+\delta_{j1}E_{i2}\}}_{\text{II}} + \underbrace{[k_j-\delta_{j2}k_1\tau][2k_1E_{i2}-Ri(k_2-k_1\tau)\tau_t E_{i\theta}]k^{-2} + [k_i-\delta_{i2}k_1\tau][2k_1E_{2j}-Ri(k_2-k_1\tau)\tau_t E_{j\theta}]k^{-2}}_{\text{III}} + \underbrace{\delta_{i2}Ri\tau_t E_{j\theta}+\delta_{j2}Ri\tau_t E_{i\theta}}_{\text{IV}} - \underbrace{\frac{2k^2E_{ij}}{\tau_t}}_{\text{V}}, \tag{1}$$

$$\underbrace{\frac{\partial E_{i\theta}}{\partial \tau}}_{\text{I}} = \underbrace{-\left\{\frac{E_{i2}}{\tau_t}+\delta_{i1}E_{2\theta}\right\}}_{\text{II}} + \underbrace{[k_i-\delta_{i2}k_1\tau][2k_1E_{2\theta}-Ri(k_2-k_1\tau)\tau_t E_{\theta\theta}]k^{-2}}_{\text{III}} + \underbrace{\delta_{i2}Ri\tau_t E_{\theta\theta}}_{\text{IV}} - \underbrace{\left[1+\frac{1}{Pr}\right]\frac{k^2E_{i\theta}}{\tau_t}}_{\text{V}}, \tag{2}$$

$$\underbrace{\frac{\partial E_{\theta\theta}}{\partial \tau}}_{\text{I}} = \underbrace{-\frac{2E_{2\theta}}{\tau_t}}_{\text{II}} - \underbrace{\frac{2k^2E_{\theta\theta}}{Pr\tau_t}}_{\text{V}}, \tag{3}$$

where E_{ij} is the spectrum function of $\overline{(u_i)_A(u_j)_B}$ at two points A and B non-dimensionalized by $\nu\tau_t/[J_0(\partial\bar{U}/\partial y)]$, $E_{i\theta}$ the spectrum function of $\overline{(u_i)_A(\theta)_B}$ non-dimensionalized by $\nu/[J_0(\partial\bar{T}/\partial y)]$, $E_{\theta\theta}$ the spectrum function of $\overline{(\theta)_A(\theta)_B}$ non-dimensionalized by $\nu(\partial\bar{U}/\partial y)/[\tau_t J_0(\partial\bar{T}/\partial y)^2]$, k the wavenumber non-dimensionalized by $[\nu\tau_t/(\partial U/\partial y)]^{\frac{1}{2}}$ $(=[k_1^2+(k_2-k_1\tau)^2+k_3^2]^{\frac{1}{2}})$, k_i the dimensionless wavenumber component in the i-direction, θ the temperature fluctuation, ν the kinematic viscosity, J_0 the constant that depends on initial conditions in the dimensional form of (4), and Pr is the Prandtl number. In (1)–(3) term I is the change per unit of time (or, in the developing steady flow, advection), term II the production by vertical uniform velocity gradient or temperature gradient, term III the pressure-force production, term IV the buoyancy production and term V is the dissipation. For solving the spectral equations (1)–(3), the turbulence is assumed to be isotropic and temperature fluctuation is assumed to be absent at a non-dimensional initial time $\tau = 0$. The conditions are satisfied by (Deissler 1958, 1967, 1971)

$$E_{ij} = \frac{1}{12\pi^2}(\delta_{ij}k^2-k_ik_j) \quad (\tau = 0), \tag{4}$$

$$E_{i\theta} = E_{\theta\theta} = 0 \quad (\tau = 0). \tag{5}$$

Under these conditions, (1)–(3) can be solved numerically by using a Runge–Kutta method. By letting the distance between two points A and B be equal to zero and integrating the spectral solutions at a terminal time τ_t over the wavenumber k-space, we can obtain the time-averaged turbulence quantities. The value of the parameter τ_t was determined to be four from the comparison with measurements of the velocity correlation values in neutral flow. Calculations were performed for Richardson numbers ranging from 0 to 0.5 and a Prandtl number of 5.

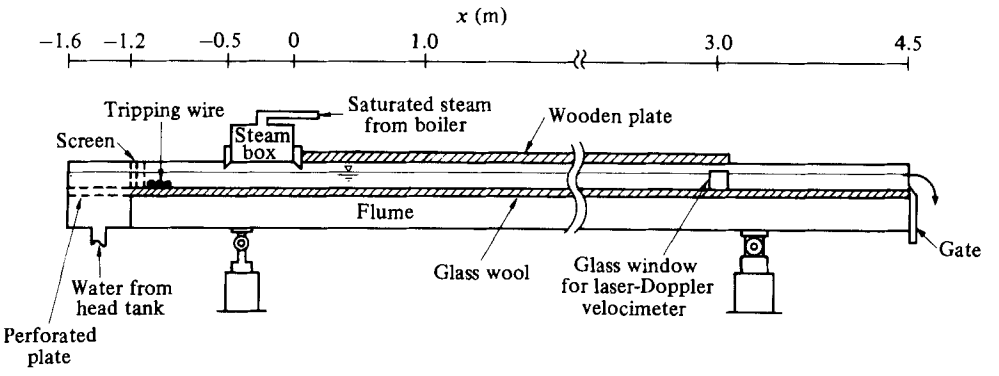

FIGURE 1. Experimental flume.

3. Experiment

The flows were set up in an open channel of square cross-section, as shown in figure 1. The inside width and the depth were 0.3 and 0.06 m respectively and the length was 6.1 m. The sidewalls and the bottom were made of smooth stainless-steel plates lined with 0.03 m thick glasswool to maintain adiabatic conditions. The details of the experimental set-up used here are described in Komori (1980) and Mizushina *et al.* (1978).

To obtain stably stratified flow, saturated steam at 373 K was mildly condensed on the free surface of the open-channel flow in the region where the flow is a fully developed turbulent flow. Steam was supplied from a steam box located at a distance 1.6 m downstream from the inlet of the flume.

The measurement station was located at the centre of the flume at a distance 3.0 m downstream ($x/\delta = 75$, δ is the flow depth) from the end of the steam box ($x = 0$). At this station the stably stratified flow was approximately in a fully developed condition. The temperature of the water recirculating through the flume was controlled to within ± 0.05 K at a fixed temperature in a temperature-regulating tank. For velocity and temperature measurements a DISA 55L laser-Doppler velocimeter (LDV) and a miniature TSI 1264 conical cold-film probe operated by a DISA 55M20 temperature bridge were used. The measuring technique and the accuracy of the velocity measured by LDV in non-isothermal flow are described in detail in an earlier paper (Mizushina *et al.* 1979). In the present experiment, the errors were estimated to be about $\pm 1\,\%$ for the mean temperature and velocity, less than $\pm 2\,\%$ for the r.m.s. values of the turbulent fluctuations, and about $\pm 3\,\%$ for the turbulent fluxes. The voltage outputs from the instruments were converted to digital signals and processed statistically by a digital computer.

Experimental conditions in the present investigation are listed in table 1. The flow depth δ was maintained at approximately 0.04 m throughout the flume, and the Reynolds numbers Re ($= 4R\overline{U}_{\mathrm{av}}/\nu$) were 9100–17 000, where R is the hydraulic radius, $\overline{U}_{\mathrm{av}}$ the cross-sectional mean velocity and ν the kinematic viscosity. The flows investigated here were fully turbulent flows under hydraulically subcritical conditions. In table 1 the bulk Richardson number $\overline{Ri}$ ($= \beta g R(\overline{T}_{\mathrm{s}} - \overline{T}_{\mathrm{b}})/\overline{U}^2_{\mathrm{av}}$) is equal to the reciprocal of the square of the densimetric Froude number, where the suffixes s and b denote the free surface and the bottom of the flume respectively. The friction velocity u^* was evaluated by the velocity-profile method (Clauser 1954). Symbols corresponding to experimental runs in table 1 will be used in the subsequent figures.

Run no.	Symbol	$\overline{Ri} \times 10^2$	Re	$\delta \times 10^2$ [m]	$R \times 10^2$ [m]	$\overline{U}_{av} \times 10^2$ [m/s]	$u^* \times 10^3$ [m/s]	$\overline{T}_s - \overline{T}_b$ [K]
I	△	0.0 (neutral)	10100	4.1	3.2	8.1	5.1	0
II	◔	1.35 (stable)	9100	4.0	3.2	7.3	4.7	1.20
III	○	2.31 (stable)	9800	4.0	3.1	7.4	4.7	1.85
IV	◐	6.39 (stable)	17000	3.9	3.1	10.4	6.1	7.22
V	●	15.3 (stable)	10500	3.9	3.1	6.9	4.3	8.32
VI	◕	19.0 (stable)	14800	3.9	3.1	7.8	4.7	10.8
VII	◒	21.3 (stable)	12600	3.8	3.1	7.4	4.5	11.2
VIII	◓	26.3 (stable)	12700	3.9	3.1	7.4	4.5	13.9
IX	◑	26.9 (stable)	14900	3.9	3.1	7.9	4.8	15.6

TABLE 1. Experimental conditions

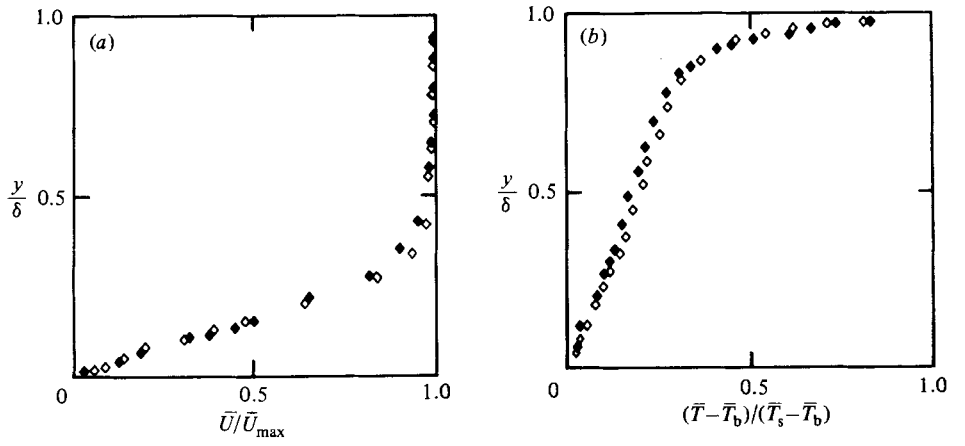

FIGURE 2. Typical distributions of the mean velocity and temperature in a strongly stable flow: ◇, $x/\delta = 75$; ◆, 63; $\overline{Ri} = 2.5 \times 10^{-2}$, $Re = 10000$.

4. Results and discussion

4.1. *Transport mechanism in stable flow*

Figure 2 shows typical distributions of the mean velocity and temperature in a strongly stable flow. In the figure, $\bar{U}_{max}$ denotes the maximum mean velocity. A temperature gradient is established in the outer layer where the velocity gradient is comparatively small and constant, and the distributions of the mean velocity and temperature do not change noticeably in the flow direction. From these facts, it can be inferred that the present flow at the measuring station is close to a developed flow.

The turbulence kinetic-energy balance equation for two-dimensional stratified flow with high Reynolds number, in which the work by the viscous shear stresses of the turbulent motion can be neglected, is given by

$$\frac{1}{2}\frac{D\overline{q^2}}{Dt} = -\overline{uv}\frac{\partial \bar{U}}{\partial y} + \beta g \overline{v\theta} - \frac{\partial}{\partial y}\left[\overline{v\left(\frac{p}{\rho} + \frac{q^2}{2}\right)}\right] - \nu\overline{\left(\frac{\partial u_i}{\partial x_j} + \frac{\partial u_j}{\partial x_i}\right)\frac{\partial u_j}{\partial x_i}}, \tag{6}$$

where $\overline{q^2}\,(= \overline{u^2} + \overline{v^2} + \overline{w^2})$ is the turbulence kinetic energy, u the velocity fluctuation in the streamwise x-direction, v the velocity fluctuation in the vertical y-direction, θ the temperature fluctuation, p the pressure fluctuation and ρ the density. The first term on the right is the shear-production term, the second the buoyancy-production term, the third the diffusion term, and the last is the viscous-dissipation term. Each term in the above equation is made dimensionless with δ/u^{*3}, and plotted against y/δ in figure 3 for a neutral flow (run I), a mildly stable flow (run V) and a strongly stable flow (run VIII) respectively. In these diagrams the viscous dissipation ϵ was estimated from the normalized power-spectral density $S_{uu}(\kappa)$ of the streamwise velocity fluctuation by using the Kolmogorov hypothesis for the inertial subrange, i.e.

$$S_{uu}(\kappa) = \alpha \epsilon^{\frac{2}{3}} \kappa^{-\frac{5}{3}},$$

where κ is the wavenumber defined by $\kappa = 2\pi n/\bar{U}$ (n is the frequency). The value of $\alpha = 0.517$, suggested by Gibson (1962), was used. The sum of the diffusion of the turbulence energy and the advection was calculated as a residue of (6) on the assumption that the flow is steady.

Under stable conditions, the shear production term is reduced significantly in the outer region. In a strongly stable flow, a small negative contribution is observed

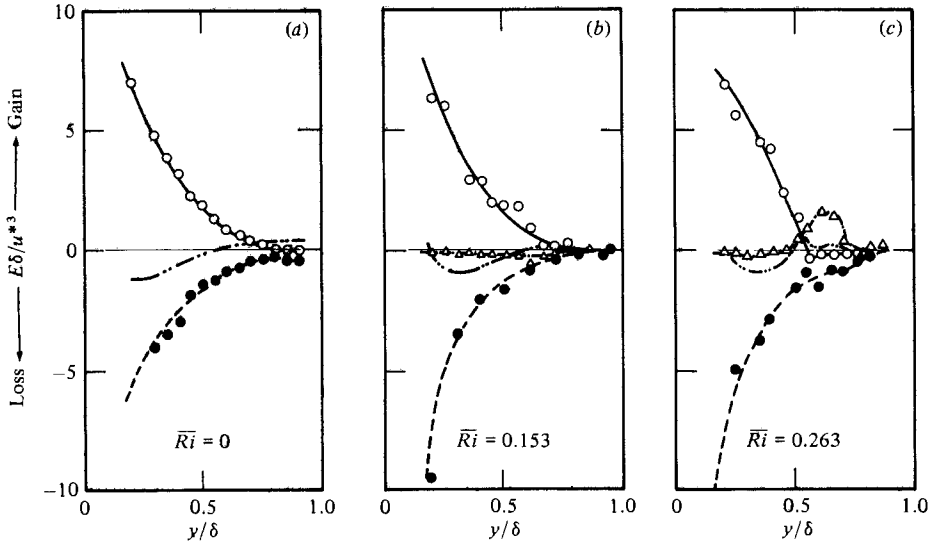

FIGURE 3. Turbulence kinetic-energy balance in stable and neutral flows: (*a*) a neutral flow (run I); (*b*) a mildly stable flow (run V); (*c*) a strongly stable flow (run VIII); —○—, shear production; – – –△– – –, buoyancy production; – –●– –, dissipation; ———. diffusion and advection.

in the region of $y/\delta \gtrsim 0.5$. This suggests that in strongly stable conditions momentum is transferred by a buoyancy-driven motion against the mean velocity gradient, which will be discussed later on. The buoyancy-production term $\beta g\overline{v\theta}$ makes a negative contribution in a mildly stable flow (run V), but in a strongly stable flow (run VIII) it makes a large positive contribution in the outer layer of $y/\delta > 0.5$. This means that the buoyancy works so as to reduce the turbulence kinetic energy in weak stratification, and that in strongly stable conditions turbulence energy is generated by upward heat transfer against the mean temperature gradient (a positive $\overline{v\theta}$). This buoyancy production is larger than the negative shear production, and the countergradient heat transfer occurs in more weakly stable conditions than the countergradient momentum transfer. The countergradient heat transfer was also observed by Piat & Hopfinger (1981) in a stratified boundary-layer flow in a wind tunnel. Although they did not explain this observation, they showed that by adding the molecular transfer the total heat flux did not change sign. In the present experiments, the countergradient momentum transfer was approximately compensated by molecular transfer, but the countergradient heat transfer greatly exceeded the molecular transfer. This suggests that in a strongly stable flow heat is supplied by advection from upstream and this heat is pumped up against the temperature gradient. The present stratified flow was obtained by steam condensation on the free surface of the open-channel flow in the region where the flow had been a fully developed flow under neutral conditions. In this flow configuration, the mean temperature gradient was first formed, and then temperature fluctuations were generated from the interactions of the mean temperature gradient with the existing velocity fluctuations. Thus, in the present strongly stable flow with a large positive temperature gradient in the outer layer, very positively skewed temperature fluctuations may be generated and may be advected downstream.

In fact, very positively skewed spikes of temperature fluctuation are observed in a simultaneous recording of θ, v and $v\theta$, as shown in figure 4. The intermittent positive spikes of θ are accompanied by positive peaks of v, and the peaks result in the positive

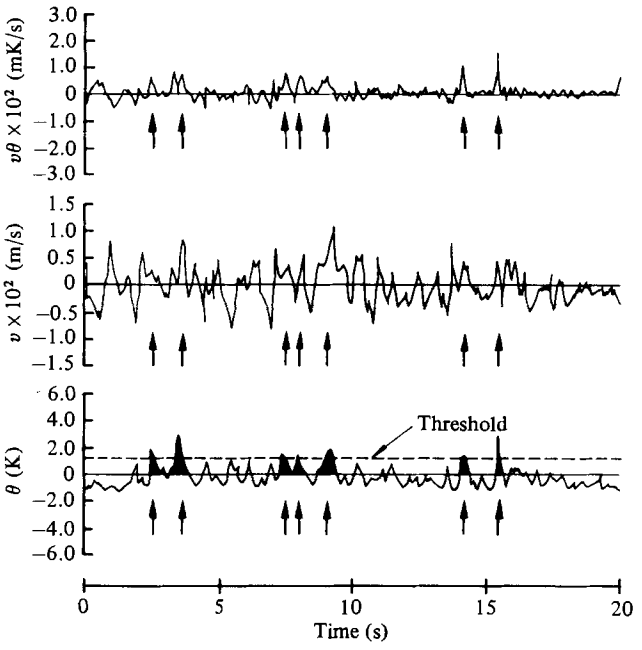

FIGURE 4. Simultaneous recording of the instantaneous values of θ, v and $v\theta$ at $Ri = 0.91$ and $y/\delta = 0.61$ in a strongly stable flow (run VIII); ----. threshold level.

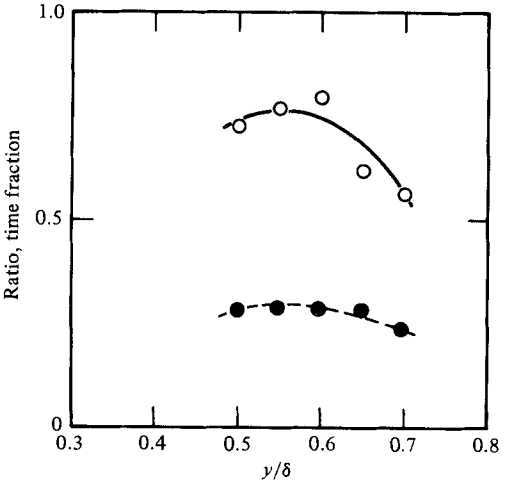

FIGURE 5. The ratio of the vertical heat flux by the intermittent upward motion of the hot eddies to the total vertical heat flux and the time fraction of the appearance of the hot eddies in a strongly stable flow (run VIII): —○—. ratio of heat flux; ---●---, time fraction.

$v\theta$-products shown by the arrows in the figure. In order to estimate the contribution of these positive $v\theta$-products to the total heat transfer, a threshold level was set with the magnitude of the r.m.s. value of θ in the θ-trace, as shown by a dashed line in figure 4. The heat flux due to the intermittent eddies with higher temperature fluctuations than the threshold level is calculated and divided by the total turbulent heat flux. The ratio and the time fraction of the appearance of intermittent eddies are plotted in figure 5. In the region of $y/\delta \gtrsim 0.7$ or $y/\delta \lesssim 0.5$, the ratio and the time

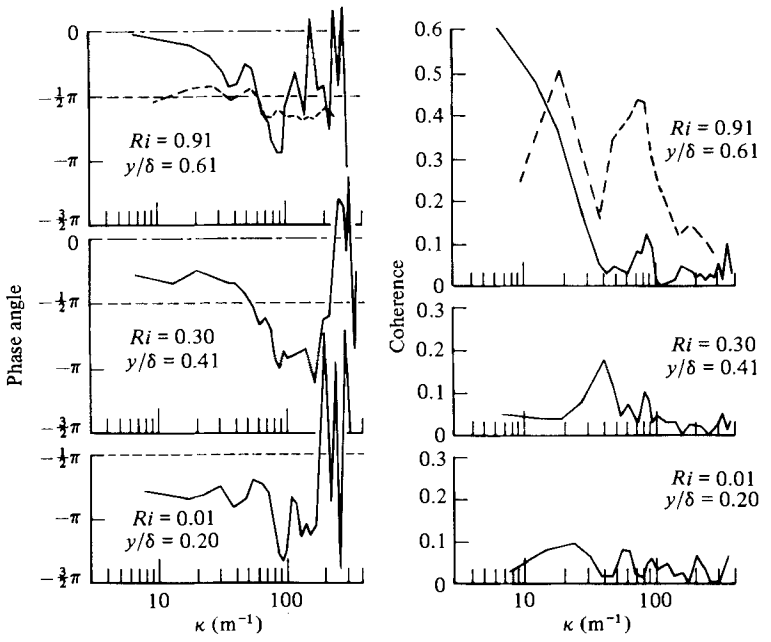

FIGURE 6. v–θ phase angles and coherences in a strongly stable flow (run VIII): ——, conventional time average; -------, conditional time average.

fraction are not plotted, since these spikes could not be distinguished in the temperature traces. Although the time fraction of the appearance of the positive spikes is less than 0.29, the ratio attains about 0.75 in the region near $y/\delta = 0.6$. This supports the assumption that intermittent upward motions of the advected eddies with the positive spikes of temperature fluctuation cause upward heat transfer against the temperature gradient. The upward motion seems to be a kind of buoyancy-driven motion, and it may trigger off a breakdown of wavelike motion under strongly stable conditions.

The presumption can also be confirmed from the velocity–temperature coherence–phase relationships. In the wave motions the v–θ coherence should be high and the phase angle should be equal to $\pm\frac{1}{2}\pi$, while the turbulent shear flow has a phase angle near $\pm\pi$ (McBean & Miyake 1972). Figure 6 shows the v–θ phase angles and coherences as a function of wavenumber κ for three positions in a strongly stable flow (run VIII). In the almost neutral region, e.g. $y/\delta = 0.2$ and $Ri = 0.01$, ordinary turbulent motions predominate, so that the phase angles are near $-\pi$ except for the range of high wavenumber. In stable stratification of $Ri = 0.3$ and $y/\delta = 0.41$, the phase angles approach $-\frac{1}{2}\pi$ and the coherences become somewhat higher in the wavenumber region of $\kappa \lesssim 50$. The phase–coherence relationships suggest that the turbulent motions become close to wavelike motions in stable conditions.

In strongly stable stratification of $Ri = 0.91$ and $y/\delta = 0.61$, the phase angles approach zero in the lower-wavenumber region and coherences become extremely high. These high coherences without phase shift show the appearance of buoyancy-driven upward motion of the hot eddy. In order to investigate the background motion during the absence of the buoyancy-driven motion, we eliminated the v- and θ-signals due to the buoyancy-driven motion by using a threshold level shown in figure 4 and conditionally calculated the phase angles and coherences. The results show that the phase angles approach $-\frac{1}{2}\pi$ and the coherences become high even in strongly stable

stratification of $Ri = 0.91$ and $y/\delta = 0.61$, as shown by a dashed line in figure 6. These suggest that also in strongly stable conditions background motion is wavelike motion and the wavelike motion is intermittently broken down by a buoyancy-driven motion of the hot eddy.

The countergradient momentum transfer may also be attributed to the buoyancy-driven motion. However, it is difficult to explain experimentally the mechanism of the countergradient momentum transfer, since the pressure effect may become significant, as discussed later on.

In figure 3 the diffusion and advection term in the outer layer of $y/\delta \gtrsim 0.4$ is small under neutral and stable conditions, and the buoyancy and shear productions are almost balanced by the viscous dissipation. However, the small diffusion and advection become comparable to or exceed the shear and buoyancy productions in the range where both the shear and buoyancy productions are close to zero. Thus the present flow is not perfectly in local equilibrium, but it will be close to a free shear flow in local equilibrium.

4.2. *Correlation of turbulence quantities with local gradient Richardson number*

The outer layer of the present flow is close to a free shear flow in local equilibrium, as mentioned above. From this fact, together with other experimental results in free shear flows (Webster 1964; Young 1975; Mizushina *et al.* 1978; Komori *et al.* 1982*a*), it is expected that Ri becomes a scaling parameter in the outer layer. The correlations of turbulence quantities with Ri are shown in figure 7, compared with the predictions of the spectral-equation model and other laboratory measurements (Webster 1964; Young 1975). Here only values measured in the outer layer of $0.4 < y/\delta < 0.75$ were adopted and correlated with Ri. In the outer layer the variations of the turbulence quantities against y/δ were very small in neutral conditions, so that the effect of y/δ were negligible.

The ratios of the root-mean-square values of the two velocity fluctuations v'/u' and w'/u' are shown, compared with the other results, where u', v' and w' are the root-mean-squares of u, v and w respectively, and w is the lateral velocity fluctuation. The ratio of v'/u' decreases slightly as the stratification shifts from neutral to weakly stable conditions and then increases as Ri becomes larger. Although these behaviours are different from Webster's and Young's measurements, the fact that vertical motions are induced more than horizontal motions under strongly stable conditions, is very interesting and can be easily understood, since the buoyancy-production term, which comes from the vertical heat flux in the $\overline{v^2}$ transport equation, has a positive contribution to $\overline{v^2}$ production (see figure 3*c*). The change of sign of $\overline{v\theta}$ is also predicted by the present spectral-equation model, and calculations of the terms in the turbulence kinetic-energy balance equation suggest that the contribution by buoyancy production becomes positive in the strongly stable condition (figure 8). In contrast with v'/u', the ratio w'/u' is almost constant in the whole range of Ri.

The correlation coefficient of the Reynolds stress $R_{uv} = -\overline{uv}/u'v'$ decreases with increasing Ri and has small negative values in the strongly stable range of $Ri > 0.7$. A similar behaviour is seen in the distribution of the correlation coefficient of the vertical heat flux $R_{v\theta} = -\overline{v\theta}/v'\theta'$, where θ' is the r.m.s. value of the temperature fluctuation θ. That is, the vertical transfers of momentum and heat are suppressed in weakly stable conditions, and in the extremely stable range of $Ri > 0.5$–0.7 they occur against their mean gradients. It can also be seen that the negative value of $R_{v\theta}$ is larger than that of R_{uv} and the change of the sign of $R_{v\theta}$ occurs in more weakly stable conditions. The present data of R_{uv} are in good agreement with the laboratory

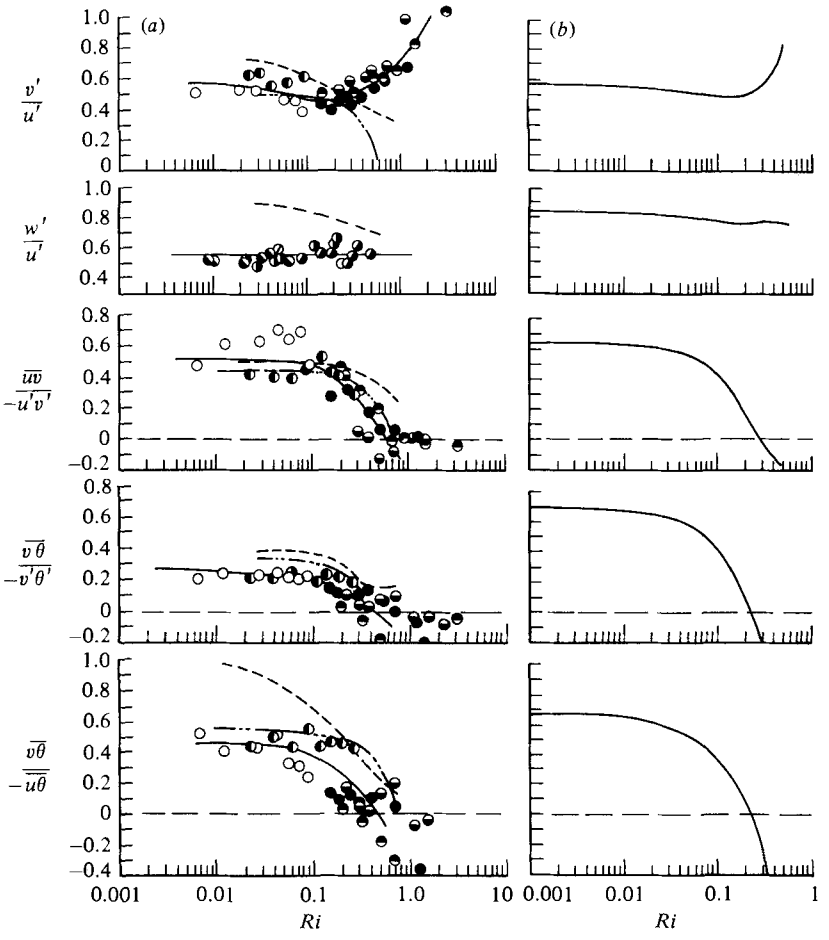

FIGURE 7. Correlation of turbulence quantities with local gradient Richardson number for $0.4 < y/\delta < 0.75$; symbols as in table 1. (*a*) Measured results: ——, best-fit curve of the present data; – – –, data of Webster (1964); – · –, data of Young (1975). (*b*) Predictions by the spectral-equation model.

measurements by Young (1975). Webster's data also show similar decreasing behaviour with stability. The zero values of R_{uv} and $R_{v\theta}$ suggest that the turbulent motion approaches wavelike motion with increasing stability. The correlation coefficients and the contribution terms in their transport equations (1) and (2) are calculated by the spectral-equation model and shown in figures 7 and 9. The calculations of the correlation coefficients are in qualitative agreement with the measured values; in particular, the prediction of the negative correlation coefficients is significant (figure 7). The predicted value of $R_{v\theta}$ attains about -0.5 at $Ri = 0.5$, although it is beyond the range of the figure. This large negative correlation seems to support the experimental results; in strongly stable conditions buoyancy-driven motions appear, so that the phase angles decrease (figure 6). From the calculations it is also found that the variations of $R_{v\theta}$ and R_{uv} are mainly due to the remarkable increase in the buoyancy term (figure 9). The buoyancy-production terms in the transport equations of $-\overline{v\theta}$ and $-\overline{uv}$ are denoted by $\beta g\overline{\theta^2}$ and $\beta g\overline{u\theta}$ respectively. The budgets of these buoyancy terms are calculated by the spectral-equation model and shown in figure 10. It can be seen that the increase of the buoyancy term $\beta g\overline{\theta^2}$ in stable

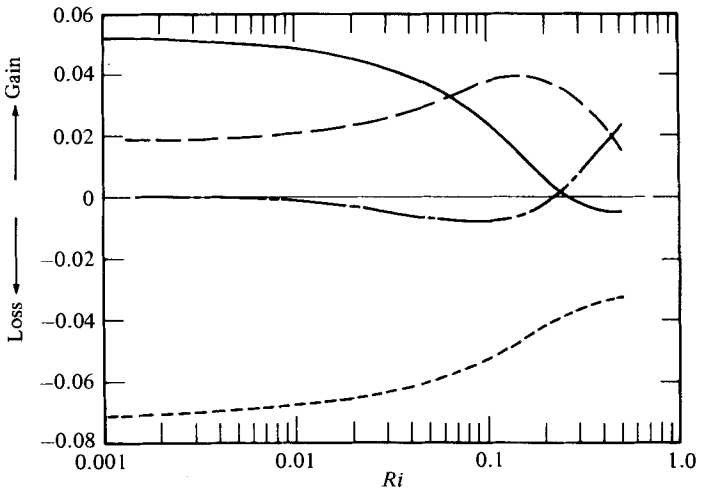

FIGURE 8. Stability dependence of the energy budget calculated from the model. Each term is non-dimensionalized by $\nu^{\frac{5}{2}}(t_t-t_0)/[J_0(\partial\overline{U}/\partial y)]$, where t_0 is the initial time, t_t the terminal time and J_0 the constant that depends on initial conditions in (4) and (5). ——, shear production; —·—, buoyancy production; – – –, dissipation; ———, advection.

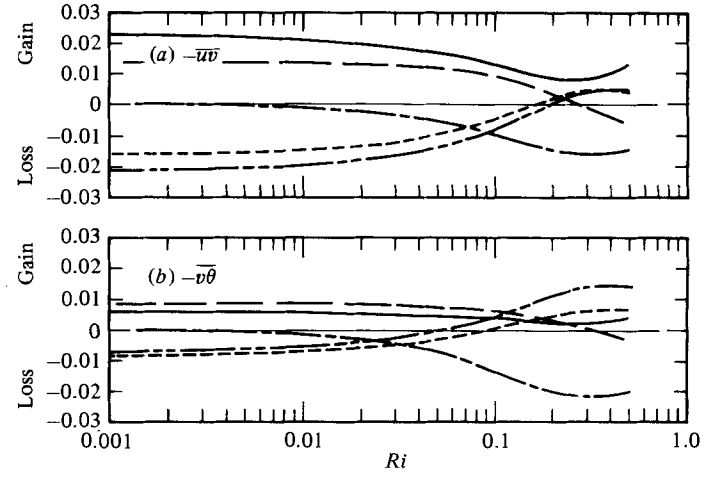

FIGURE 9. Stability dependence of the budgets of shear stress and heat flux calculated from the model: (*a*) budget of the shear stress non-dimensionalized by $\nu^{\frac{5}{2}}(t_t-t_0)^{\frac{7}{2}}/[J_0(\partial\overline{U}/\partial y)]$; (*b*) budget of the vertical heat flux non-dimensionalized by $\nu^{\frac{5}{2}}(t_t-t_0)^{\frac{3}{2}}/[J_0(\partial\overline{U}/\partial y)(\partial\overline{T}/\partial y)]$; ——, mean-field production; – – –, buoyancy production; —·—, pressure-force production; – – –, dissipation; ———, advection.

conditions is attributed to the contribution of the advection term. In the present model, a constant temperature gradient is first formed in the existing isotropic field at an initial time, and then the temperature fluctuations are produced by the interactions of the mean temperature gradient with the turbulence (Deissler 1967). This situation is similar to that of the present experiment, and also in the case of the model very large temperature fluctuations will be generated from a large positive temperature gradient in strongly stable conditions. The eddies (parcels) with the large temperature fluctuations are advected (see the increase of the advection term in figure 10) and then they are driven by buoyancy. These buoyancy-driven motions result in the upward heat transfer against the temperature gradient, i.e. a positive $\overline{v\theta}$.

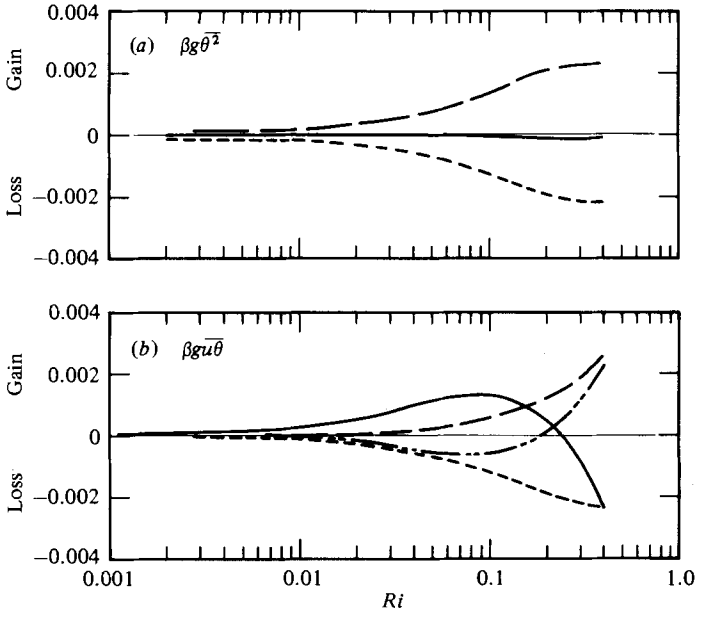

FIGURE 10. Stability dependence of the budgets of buoyancy production terms calculated from the model: (*a*) budget of $\beta g\overline{\theta^2}$ non-dimensionalized by $\nu^{\frac{5}{2}}(t_t-t_0)\,(\partial\overline{U}/\partial y)^2/[J_0(\partial\overline{T}/\partial y)]$; (*b*) budget of $\beta g\overline{u\theta}$ non-dimensionalized by $\nu^{\frac{5}{2}}(t_t-t_0)^{\frac{3}{2}}\,(\partial\overline{U}/\partial y)^2/J_0$; ——, mean-field production; — — —, buoyancy production; —·—, pressure-force production; – – –. dissipation; ———, advection.

The increase in the buoyancy production term $\beta g\overline{u\theta}$ in the transport equation of $-\overline{uv}$ is attributed to the increase in both the advection and pressure-force production terms (figure 10). The pressure-force term works so as to reduce $-\overline{uv}$ in weakly stable conditions, whereas in strongly stable conditions it makes a large positive contribution. Although the mechanism of the interactions between pressure and temperature is not clear, this behaviour of the pressure-force term may also be caused by the buoyancy-driven motions mentioned above.

The ratio $-\overline{v\theta}/\overline{u}$ of the vertical to the streamwise heat flux decreases rapidly with increasing stability and ultimately crosses the zero value. Except under strongly stable conditions, the present behaviour is in good agreement with Young's and Webster's data. The behaviour predicted by the spectral-equation model is also in qualitative agreement with the present measurements (figure 7).

5. Conclusions

Buoyancy effects on the turbulence structure in the outer layer of stably stratified open-channel flow have been investigated experimentally and a theoretical consideration has been added. The main results from this study can be summarized as follows.

(1) The outer layer of the present flow is close to local equilibrium, and there the local gradient Richardson number Ri becomes a significant parameter for representing the buoyancy effects. Turbulence quantities in stable conditions are well correlated with Ri, and their variations with Ri are qualitatively predicted by a spectral-equation model based on two-point correlation equations.

(2) In stable conditions, fluctuating motions become close to wavelike motions, and turbulent heat and momentum transfer against the mean temperature and velocity gradients occurs in strongly stable stratification. Especially, the countergradient heat

transfer in the vertical direction is remarkable, and it is due to the intermittent buoyancy-driven motions: in the present flow configuration, the intermittent upward motions of the advected eddies with higher temperature than the mean temperature.

REFERENCES

Arya, S. P. S. 1975 *J. Fluid Mech.* **68**, 321.

Arya, S. P. S. & Plate, E. J. 1969 *J. Atmos. Sci.* **26**, 656.

Clauser, F. H. 1954 *J. Aero. Sci.* **21**, 91.

Deissler, R. G. 1958 *Phys. Fluids* **1**, 111.

Deissler, R. G. 1967 *NASA* TN D-3999, 1.

Deissler, R. G. 1971 *Z. angew. Math. Phys.* **22**, 267.

Ellison, T. H. & Turner, J. S. 1960 *J. Fluid Mech.* **8**, 514.

Gibson, M. M. 1962 *Nature* **195**, 1281.

Gibson, M. M. & Launder, B. E. 1978 *J. Fluid Mech.* **86**, 491.

Haugen, D. A., Kaimal, J. C. & Bradley, E. F. 1971 *Q. J. R. Met. Soc.* **97**, 168.

Komori, S. 1980 Ph.D. dissertation., Kyoto University.

Komori, S., Ueda, H., Ogino, F. & Mizushina, T. 1982*a* In *Heat Transfer* 1982, vol. 2, p. 431. Hemisphere.

Komori, S., Ueda, H., Ogino, F. & Mizushina, T. 1982*b* *Phys. Fluids* **25**, 1359.

Launder, B. E. 1975 *J. Fluid Mech.* **67**, 569.

McBean, G. A. & Miyake, M. 1972 *Q. J. R. Met. Soc.* **98**, 383.

Mizushina, T., Ogino, F., Ueda, H. & Komori, S. 1978 In *Heat Transfer* 1978, vol. **1**, p. 91. Hemisphere.

Mizushina, T., Ogino, F., Ueda, H. & Komori, S. 1979 *Proc. R. Soc. Lond.* **A366**, 63.

Piat, J. F. & Hopfinger, E. J. 1981 *J. Fluid Mech.* **113**, 411.

Schiller, E. J. & Sayre, W. W. 1975 *J. Hydraul. Div. A.S.C.E.* **101** (HY 6), 749.

Ueda, H., Mitsumoto, S. & Komori, S. 1981 *Q. J. R. Met. Soc.* **107**, 561.

Webster, C. A. G. 1964 *J. Fluid Mech.* **19**, 221.

Wyngaard, J. C., Cote, O. R. & Izumi, Y. 1971 *J. Atmos. Sci.* **28**, 1171.

Young, S. T. B. 1975 *Queen Mary Coll., London, Rep.* QMC-EP6018.